

Characterization of Collagen Thin Films for von Willebrand Factor Binding and Platelet Adhesion

Ryan R. Hansen,[†] Alena A. Tipnis,[†] Tara C. White-Adams,[‡] Jorge A. Di Paola,[‡] and Keith B. Neeves^{*,†,‡}

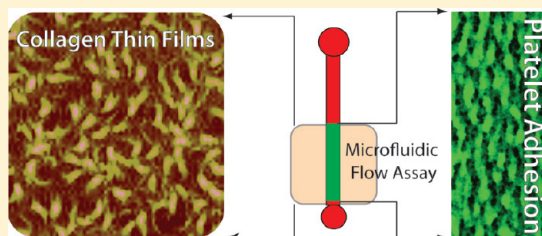
[†]Department of Chemical and Biological Engineering, Colorado School of Mines, Golden, Colorado 80401, United States

[‡]Department of Pediatrics, University of Colorado, Aurora, Colorado 80045, United States

S Supporting Information

ABSTRACT: Von Willebrand factor (VWF) binding and platelet adhesion to subendothelial collagens are initial events in thrombus formation at sites of vascular injury. These events are often studied *in vitro* using flow assays designed to mimic vascular hemodynamics. Flow assays commonly employ collagen-functionalized substrates, but a lack of standardized methods of surface ligation limits their widespread use as a clinical diagnostic. Here, we report the use of collagen thin films (CTF) in flow assays. Thin films were grown on hydrophobic substrates from type I collagen solutions of increasing concentration (10, 100, and 1000 $\mu\text{g}/\text{mL}$).

We found that the corresponding increase in fiber surface area determined the amount of VWF binding and platelet adhesion. The association rate constant (k_a) of plasma VWF binding at a wall shear stress of 45 dyn/cm^2 was 0.3×10^5 , 1.8×10^5 , and $1.6 \times 10^5 \text{ M}^{-1} \text{ s}^{-1}$ for CTF grown from 10, 100, and 1000 $\mu\text{g}/\text{mL}$ solutions, respectively. We observed a 5-fold increase in VWF binding capacity with each 10-fold increase in collagen solution concentration. The association rates of Ser1731Thr and His1786Asp VWF mutants with collagen binding deficiencies were 9% and 22%, respectively, of wild-type rates. Using microfluidic devices for blood flow assays, we observed that CTF supported platelet adhesion at a wall shear rate of 1000 s^{-1} . CTF grown from 10 and 100 $\mu\text{g}/\text{mL}$ solutions had variable levels of platelet surface coverage between multiple normal donors. However, CTF substrates grown from 1000 $\mu\text{g}/\text{mL}$ solutions had reproducible surface coverage levels ($74 \pm 17\%$) between normal donors, and there was significantly diminished surface coverage from two type 1 von Willebrand disease patients (8.0% and 24%). These results demonstrate that collagen thin films are homogeneous and reproducible substrates that can measure dysfunctions in VWF binding and platelet adhesion under flow in a clinical microfluidic assay format.



INTRODUCTION

Following a vascular injury, bleeding is arrested by platelets that first adhere to the exposed subendothelial matrix and then aggregate to form a hemostatic plug. It is well-recognized that shear stress plays a critical role in this process.¹ As such, *in vitro* methods of characterizing platelet function under physiological shear stress offer potential in improving the diagnoses and treatment of platelet adhesion disorders such as von Willebrand disease (VWD), which is often difficult to categorize into clinically relevant phenotypes.² Over the past 30 years, flow assays to measure platelet function have been developed toward this application in the format of annular or parallel plate flow chambers,^{3–7} or more recently, microfluidic formats that minimize volume and increase throughput.^{8,9} Common to all flow assays is the necessity of functionalizing a substrate with adhesive proteins capable of capturing and activating platelets under flow. However, a repeatable, standardized adhesive substrate remains poorly defined, limiting interpretation of data between laboratories and adoption into the clinical setting.¹⁰

The most common adhesive proteins used in flow assays are extracellular matrix (ECM) proteins such as types I, III, and VI collagens and laminin, and plasma proteins such as fibrinogen,

fibronectin, and von Willebrand factor (VWF).^{11,12} At low shear stresses ($<15 \text{ dyn}/\text{cm}^2$), platelets can interact directly with collagens through two receptors, glycoprotein VI and the integrin $\alpha_2\beta_1$.^{13,14} At high shear stresses ($>15 \text{ dyn}/\text{cm}^2$), such as those encountered in the major arteries, plasma derived VWF assembles on collagens at the site of a vascular injury, allowing platelets to first roll over VWF before firmly adhering to collagen.¹⁵ The source and the preparation of collagens in flow assays has long been a cause of controversy in the hemostasis field.^{16,17} The most widely used substrates are types I and III insoluble fibrillar collagen. These insoluble collagens are potent platelet agonists and considered the most physiological in terms of their macromolecular structure.¹⁶ Drawbacks of insoluble collagens include heterogeneity in the size and type of fibers,¹ impurities within the solution (including VWF),¹⁸ and difficulty in defining a repeatable surface at the submillimeter scale, which limits its use, especially in microfluidic assays.⁸

Received: June 23, 2011

Revised: August 30, 2011

Published: October 03, 2011

Table 1. Notation and Experimental Conditions of Collagen Surface Preparations^a

notation	collagen	incubation concentration ($\mu\text{g}/\text{mL}$)	dilution buffer
CTF10	Type I bovine, acid soluble	10	1 \times PBS, pH 7.4
CTF100	Type I bovine, acid soluble	100	1 \times PBS, pH 7.4
CTF1000	Type I bovine, acid soluble	1000	1 \times PBS, pH 7.4
MC	Type I bovine, acid soluble	1000	5% glucose, pH 2.7
IC	Type I equine, insoluble	100, 250, 500	5% glucose, pH 2.7

^aAll surfaces were incubated at room temperature for 1 h, rinsed in dilution buffer, and dried.

There have been recent efforts to improve the reproducibility of collagen preparations for a variety of biological assays while achieving control over surface features, ligand densities, and molecular composition. One such approach is the use of reconstituted collagen fibers.^{19,20} This material can be deposited onto both hydrophobic and hydrophilic surfaces through the self-assembly of collagen monomers into fibers at the solid–liquid interface.^{20,21} This process is initiated by neutralizing a solution of acid-solubilized or pepsin-digested collagen monomers. The resulting collagen thin films (CTF) have been applied in investigations of adhesion and spreading of vascular smooth muscle cells,²² endothelial cells,²³ and fibroblasts.²⁴

In this study, we report the application of CTF for measuring VWF–collagen binding and platelet–collagen adhesion under arterial shear stresses. We examined the role of pH and collagen concentration on thin film properties and function. Surface features of thin films were determined by atomic force microscopy (AFM), profilometry, and surface plasmon resonance (SPR). Our results show that collagen thin films are a homogeneous substrate at the micrometer length scale and can support VWF binding and platelet adhesion under physiologically relevant shear stress. We found that VWF association rates and binding levels, and platelet adhesion levels, can be manipulated by altering the thin film properties. Finally, as a demonstration of the potential clinical utility of these substrates, we were able to detect collagen-binding deficiencies in VWF and platelet adhesion deficiencies in flow assays using blood from type I VWD patients. Taken together, these studies move toward a standardized approach of substrate preparations for flow assays measuring hemostatic function.

EXPERIMENTAL SECTION

Materials. Type I equine tendon insoluble collagen was obtained from Chrono-log Corporation. Acid-solubilized type I bovine collagen and all chemicals were purchased from Sigma-Aldrich unless noted otherwise. Antihuman CD41a – PE/Cy5 antibody was obtained from BD Pharmingen and used to label platelets in whole blood. Abciximab, an $\alpha_{\text{IIb}}\beta_3$ antagonist (ReoPro, Eli Lilly), was obtained from University of Colorado Hospital pharmacy and used in whole blood. Prostacyclin was obtained from Cayman Chemical Co. Human plasma VWF was obtained from Haematologic Technologies Inc. Recombinant VWF samples expressed in human embryonic kidney (HEK) 293T cells following site-directed mutagenesis using the Stratagene QuikChange kit (Stratagene, La Jolla, CA, USA) were received from Dr. Veronica Flood at the BloodCenter of Wisconsin. Recombinant VWF samples included wild type (wt) VWF, French Ser1731Thr, and His1786Asp VWF constructs.²⁵ Recombinant VWF samples were concentrated using ultrafiltration devices with a 100 kDa nominal molecular weight limit (Millipore) and then quantified with an ELISA. All VWF samples were stored at $-80\text{ }^\circ\text{C}$ until use. Purified mouse antihuman-VWF (BD Pharmingen) and Alexa Fluor 488 conjugated goat antihuman IgG

(Invitrogen) were used for immunofluorescence VWF studies. Phosphate buffered saline (PBS, pH 7.4), HEPES buffered saline (HBS, pH 7.2), and Tyrode's buffer (pH 7.3) were made in-house.

Preparation of Collagen Surfaces. Collagen preparations were performed on hydrophobic glass surfaces because these surfaces best promote rapid fiber polymerization.²⁶ A few preparations were performed on clean glass as a comparison. Standard glass slides (25 mm \times 75 mm, Fisher) or circular coverslips (22 mm, Fisher) were made hydrophobic by treatments with octadecyltrichlorosilane (OTS) according to established protocols.²⁷ Briefly, slides were cleaned in solution of 1:1 methanol/hydrochloric acid (37 N) for 1 h, incubated in 1 mM OTS in anhydrous toluene for 45 min, rinsed and sonicated in toluene, and dried. AFM and X-ray photoelectron spectroscopy were used to verify the presence of a uniform 3–4 nm monolayer of OTS. Hydrophobic SPR sensor surfaces were prepared by stripping unfunctionalized gold sensor surfaces (GE Healthcare Lifesciences) with piranha solution (3:1 $\text{H}_2\text{SO}_4/\text{H}_2\text{O}_2$) for 1 h and then functionalizing with a 1-octadecane thiol monolayer according to an established protocol.²⁸

Five different collagen surface preparations were included in these studies: collagen thin films (CTF) deposited at collagen solution concentrations of 10, 100, and 1000 $\mu\text{g}/\text{mL}$, monomeric collagen (MC), and insoluble collagen (IC). Table 1 lists the notation and experimental conditions of each of the five preparations. CTFs were obtained by neutralizing acid soluble collagen with 0.1 M NaOH and then dilution into 1 \times PBS, followed by incubation on OTS functionalized substrates for 1 h, rinsed five times in 1 \times PBS, rinsed thoroughly in deionized water, and quickly dried. We used compressed air to rapidly remove any water and dry the surface in less than one minute. MC and IC surfaces were obtained by dilution of acid-solubilized collagen or type I equine tendon insoluble collagen, respectively, into 5% glucose solution, pH 2.7, using identical surface incubation conditions. IC surfaces were used to draw comparisons to CTFs, as typical flow assays use type I equine tendon insoluble collagen to clean glass substrates at 100 $\mu\text{g}/\text{mL}$ concentrations.²⁹

Characterization of Collagen Surfaces. A Nanoscope III AFM was used to image dehydrated collagen thin films. Silicon cantilevers with reflective Al coating and a resonance frequency of 320 kHz and 42 N/m spring constant (TESPA probes, Veeco) were used in tapping mode. Scan areas were varied between 1 and 144 μm^2 . All images were captured at a scan rate between 1 and 2.5 Hz. Fiber thicknesses, surface roughness, and fiber surface area were analyzed with Veeco software. All images were normalized to account for sample tilt and baseline drift using the “Flatten” function in the Veeco software. Fiber thickness was determined by height profiles and measured for 25–50 fibers per image in three different areas on the film. A surface profilometer (Tencor P-10) was used to obtain film thicknesses of dehydrated collagen surfaces. Three to five separate preparations were used for each film thickness measurement. Stylus force was set at a minimum (1 mg) to minimize damage of collagen upon contact with the stylus tip. Collagen ligand density measurements were performed with SPR (BiaCore 3000 instrument). Alkane-thiol modified sensors were read in the SPR prior to thin film functionalization to determine background response units (RU) generated from each individual sensor in the BiaCore, and again measured after thin film deposition. An increase in 1000 RU

corresponds to a 1 ng/mm^2 ligand surface density,³⁰ and each ligand was taken to be 310 kDa, the molecular weight of tropocollagen.³¹ Four separate measurements were taken for each thin film preparation.

Measurement of VWF Adsorption Kinetics to Collagen Surfaces. The association and dissociation kinetics of VWF onto collagen thin films under flow was measured by SPR. All collagen-functionalized SPR surfaces were blocked with 5 mg/mL BSA for 45 min, loaded into the BiaCore instrument, and primed with degassed $1 \times \text{PBS}$ for 18 min to achieve a steady baseline signal. Serial dilutions of native plasma VWF were made in degassed $1 \times \text{PBS}$ to concentrations of 30, 40, 60, 120, and 240 nM, assuming VWF to be monomeric ($M_r = 250 \text{ kDa}$), and the VWF solutions were perfused over the CTF substrates at a flow rate of $10 \mu\text{L}/\text{min}$. This flow rate corresponds to a wall shear stress of 45 dyn/cm^2 within the channel (inner channel dimensions: $20 \mu\text{m} \times 500 \mu\text{m} \times 2300 \mu\text{m}$). Recombinant VWF solutions were diluted to 1 IU/mL in a 10 w/v % Ficoll (GE Biosciences) solution, allowing for a 5-fold increase in viscosity. Recombinant VWF solutions were then perfused over CTF substrates at a flow rate of $2 \mu\text{L}/\text{min}$, corresponding to a wall shear stress of 45 dyn/cm^2 .

Analysis of association and dissociation rates was performed at each VWF concentration using *BLAevaluation* software version 4.1.1 to fit each kinetic curve. Prior to fitting, each curve was adjusted to account for baseline drift. Jumps in the signal associated with changes in buffer solutions were ignored in the analysis. Nonspecific binding of VWF to the surface was accounted for by running perfusions of VWF at each concentration over surfaces containing no collagen and then subtracting this signal from each perfusion plot in which collagen was present. Association and dissociation curves were fit separately using a 1:1 Langmuir binding model.

Blood Collection and Preparation of Washed Platelets. Phlebotomy was conducted in accordance with the Declaration of Helsinki and under the University of Colorado, Boulder Institutional Review Board approval. Human blood was collected from healthy donors via venipuncture. Donors had not consumed alcohol within 48 h prior, nor had they taken any prescription or over-the-counter drugs within 10 days. For preparation of washed platelets, 40 mL of blood was drawn into sodium citrate and 1:10 v/v acid/citrate/dextrose (ACD) and centrifuged at 200 g for 20 min to obtain platelet rich plasma (PRP). To remove plasma components, $0.1 \mu\text{g}/\text{mL}$ prostacyclin was added to PRP followed by centrifugation at 1000 g for 10 min to obtain platelet pellets. Platelets were resuspended in Tyrode's buffer with ACD and $0.1 \mu\text{g}/\text{mL}$ prostacyclin, centrifuged a second time, and finally resuspended in Tyrode's buffer. Platelet counts were obtained with a hemocytometer. For use of whole blood in the microfluidic assay, the first 8 mL of blood was drawn into an empty vacutainer and discarded, the next 5 mL was drawn into vacutainers containing 75 mM of the thrombin inhibitor Phe-Pro-Arg-chloromethylketone (PPACK) (Haematologic Technologies, Inc.). A comparison of markers for platelet activation (P-selectin and PAC-1) by flow cytometry showed no difference between vacutainer and syringe withdrawal of blood (Supporting Information Table 1). The blood was then incubated for 10 min with a non-function-blocking antihuman CD41a-PE/Cy5 antibody (platelet labeling) in the absence or presence of abciximab ($\alpha_{\text{IIb}}\beta_3$ inhibitor), to a final concentration of 20 and $40 \mu\text{g}/\text{mL}$, respectively.

Platelet Aggregometry. Platelet aggregation was monitored in citrated whole blood using a Chrono-log whole blood aggregometer according to standardized protocols. Chrono-lume (Chrono-Log Corp., Havertown, PA, USA) was added to whole blood according to manufacturer's instructions, to monitor ATP release due to platelet dense granule release. Platelet agonists included (1) acid-solubilized collagen after neutralization with 0.1 M NaOH and dilution to $1000 \mu\text{g}/\text{mL}$ in $1 \times \text{PBS}$ for 1 h to allow for bulk reconstitution of fibers [after 1 h, reconstituted fibers were further diluted to the desired concentrations (2 to $15 \mu\text{g}/\text{mL}$) and used as an agonist], (2) monomeric collagen obtained by dilution of

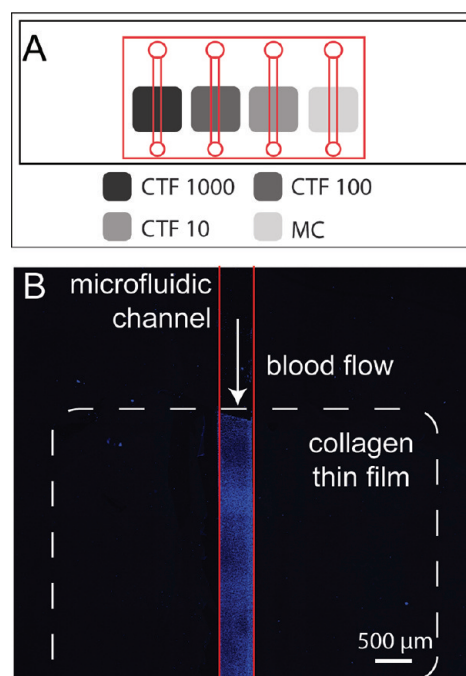


Figure 1. (A) Layout of microfluidic device (red lines) over substrates containing four patterned collagen preparations (gray boxes, see Table 1 for notation) on a glass slide (black rectangle). The device allows for simultaneous perfusions of plasma VWF or whole blood over each preparation. (B) Laser scanning confocal microscopy image of platelets (blue) adhered to CTF1000 (white dotted line) after a whole blood perfusion through a microfluidic device (red line).

acid-solubilized collagen into glucose buffer (pH 2.7) to $15 \mu\text{g}/\text{mL}$, and (3) Chono-log collagen (type I equine tendon insoluble collagen) diluted in glucose buffer (pH 2.7) to $5 \mu\text{g}/\text{mL}$.

Static Platelet Adhesion to Collagen Surfaces. OTS-modified 22-mm-diameter coverslips functionalized with CTFs were blocked with 5 mg/mL BSA for 1 h, followed by rinsing with $1 \times \text{PBS}$. Washed platelets were diluted to 2×10^7 platelets/mL in Tyrode's buffer and incubated onto coverslips at 37°C for 45 min. As a negative control, washed platelets treated with $20 \mu\text{g}/\text{mL}$ abciximab ($\alpha_{\text{IIb}}\beta_3$ inhibitor) were also incubated onto the CTFs, as $\alpha_{\text{IIb}}\beta_3$ integrin activation and signal transduction are required for platelet spreading.³² Surfaces were then rinsed in $1 \times \text{PBS}$, fixed with 4% formaldehyde for 10 min, permeabilized with 0.1% Triton-X 100 for 10 min, and stained with $0.1 \mu\text{g}/\text{mL}$ FITC-Phalloidin overnight at 4°C . Coverslips were imaged with a $60\times$ oil objective with an inverted epifluorescence microscope (IX81, Olympus). Three separate experiments were performed for each condition.

Measurement of Platelet Adhesion Levels onto Collagen Surfaces. Whole blood was perfused over collagen thin films at controlled wall shear rates through polydimethylsiloxane (PDMS) microfluidic devices. Each microfluidic device consisted of four channels ($500 \mu\text{m}$ wide, $50 \mu\text{m}$ high) to allow for simultaneous perfusion of whole blood over four different collagen thin film preparations. PDMS microfluidic devices were fabricated using conventional soft lithography methods according to previous protocols.³³ Prior to use, devices were cleaned with 1 N HCl, followed by sonication with acetone and ethanol, and then incubated in a 5 mg/mL BSA solution for 45 min to prevent nonspecific adsorption of blood components. Collagen solutions were incubated onto specific $7 \text{ mm} \times 7 \text{ mm}$ regions of hydrophobic glass substrates using a multiwell incubation chamber (Cat# 10486001/10486081, Whatman Inc.). Following thin film deposition, the slide was removed from the incubation chamber and blocked in 5 mg/mL BSA solution for 45 min. Following thorough rinsing and

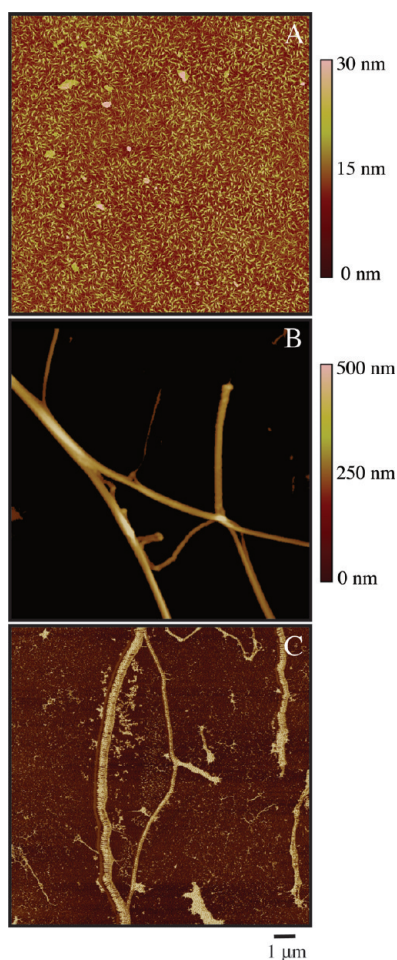


Figure 2. AFM images of (A) CTF 1000 substrate in tapping mode, (B) IC substrate in tapping mode, and (C) IC substrate in phase contrast mode. Surfaces were dried rapidly after deposition and washing and imaged in air.

drying of the slides, microfluidic devices were reversibly sealed to the slides using vacuum assisted bonding.⁸ A syringe pump (PHD 2000, Harvard Apparatus) was used with four 250 μL glass syringes (Hamilton) to pull fluid through the channels at a constant volumetric flow rate. Wall shear rate was related to volumetric flow rate through the following correlation:

$$\gamma_{\text{wall}} = \frac{(f\text{Re})Q}{2A^{1.5}} \quad (1)$$

$$f\text{Re} = \frac{12}{\left[1 - \frac{192}{\pi^5} \varepsilon \tanh\left(\frac{\pi}{2\varepsilon}\right) (1 + \varepsilon)\sqrt{\varepsilon}\right]} \quad (2)$$

where γ_{wall} is the wall shear rate, Q is the volumetric flow rate, A is the channel cross sectional area, f is the Fanning friction factor, Re is the Reynolds number, and ε is the channel aspect ratio (width/height). A schematic of the microfluidic setup is shown in Figure 1A.

Image Acquisition and Analysis. Whole blood was perfused through each channel for 5 min, followed by a 2 min perfusion of HBS to remove the whole blood and then a 5 min perfusion of 2.5% glutaraldehyde in HBS for chemical fixation of platelets. The microfluidic devices were removed from the substrates and the surfaces were coverslipped using a 70% glycerol solution in water. Platelet accumulation on

coverslipped slides was measured by confocal microscopy (Olympus Flouview FV1000) using a 647 nm laser excitation source (Figure 1B). Five separate areas ($420 \mu\text{m} \times 420 \mu\text{m}$) positioned 1, 2, 3, 4, and 5 mm downstream of the edge of the collagen were imaged using $10\times$ objective. Regions where whole blood contacted the surface upstream of the collagen films were also imaged to monitor for nonspecific platelet adhesion. Platelet surface coverage levels for each donor were calculated using a custom *Matlab* routine that thresholds each image using the triangle method.³⁴

Statistical Analysis of Data. CTF morphology measurements and platelet adhesion data are reported as the mean \pm standard deviation from repeated measurements. Differences in platelet surface coverage between different collagen preparations was determined by the Mann–Whitney U-test with $\alpha = 0.01$. Error in kinetic rate constants from SPR experiments is reported as standard error from nonlinear regression.

RESULTS

Surface Characterization of Collagen Thin Films on Microfluidic Substrates. The following acronyms are used to refer to the five surfaces used in this study: CTF10, CTF100, and CTF1000 are collagen thin films (CTFs) grown from solutions of 10, 100, and 1000 $\mu\text{g}/\text{mL}$ of type I bovine acid solubilized collagen at pH 7.4. MC is nonpolymerized or monomeric type I bovine acid solubilized collagen at pH 2.7; these substrates are used as a negative control for the role of supramolecular assembly of collagen fibers, which have been shown necessary to promote sufficient levels of platelet adhesion under flow.^{1,16} IC is insoluble type I equine collagen for comparison to a conventional flow assay substrate.

CTFs were grown on hydrophobic glass substrates for 1 h at a pH of 7.4. These conditions promote rapid self-assembly of collagen fibers at the liquid–solid surface compared to bulk fiber formation and subsequent gelation.^{21,26,35} AFM images show a dense, homogeneous film of fibers at the length scale ($\sim 1 \mu\text{m}$) of a single platelet (Figure 2A). The surface consists of a dense bed of small fibers with diameters less than 30 nm. Larger fibers (200–250 nm diameter) reported in similar systems for polymerization times of 18 h remain largely absent on the surface due to the short polymerization time.²²

For comparison to CTFs, IC substrates were used as a positive control because they are commonly used as an adhesive substrate for VWF binding and platelet adhesion flow assays.^{11,16,36,37} In contrast to CTFs, AFM images of IC substrates reveal a sparsely coated surface of discrete, banded fibers (Figure 2B). IC substrates coated with 100, 250, and 500 $\mu\text{g}/\text{mL}$ IC solutions had varied and incomplete levels of fiber surface coverage across the area of the substrate ($12 \pm 7\%$, $18 \pm 10\%$, and $64 \pm 23\%$, respectively). Additionally, the surface appears heterogeneous at the micrometer length scale with respect to fiber diameter ($260 \pm 105 \text{ nm}$, $n = 350$ fibers) and surface coverage. A phase contrast image qualitatively shows the distribution in fiber sizes (Figure 2C).

The thin film properties of CTFs deposited onto surfaces at varied concentrations (10, 100, and 1000 $\mu\text{g}/\text{mL}$) were also measured. AFM images show that each CTF substrate yields a surface consisting of a bed of collagen ligands with fibrillar morphologies (Figure 3A,C,D). AFM images of MC substrates yield a surface of amorphous aggregates ($\sim 50 \text{ nm}$) that lack a supramolecular fibrous structure, as expected since fibers do not self-assemble at low pH (Figure 3B). Table 2 summarizes the measured thin film properties of each preparation. Apparent in

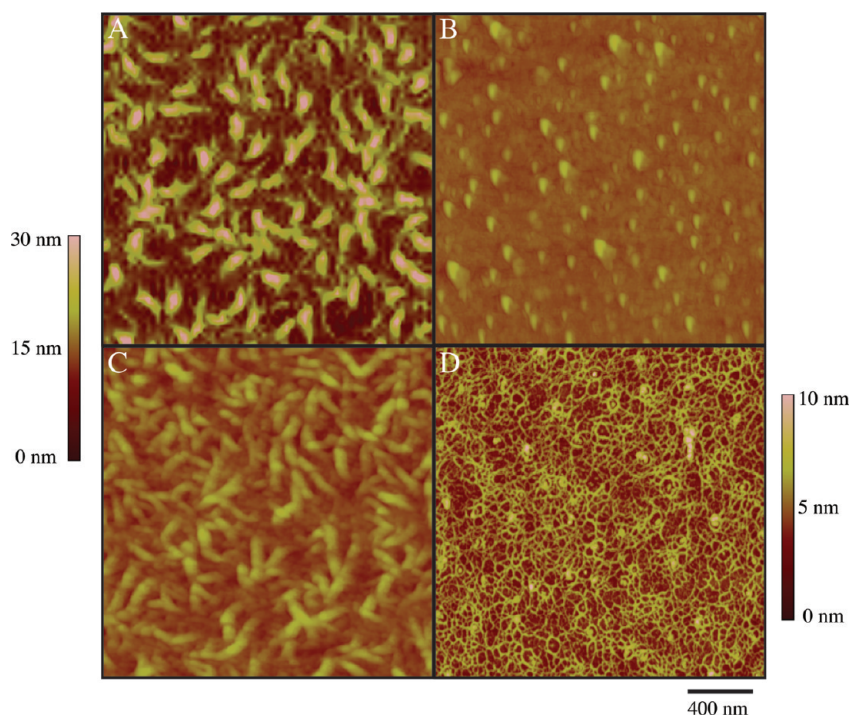


Figure 3. AFM images of collagen-functionalized substrates deposited on OTS-modified glass with a 1 h deposition time: (A) CTF1000 substrate, (B) MC substrate, (C) CTF100 substrate, and (D) CTF10 substrate. Scan sizes are $2\ \mu\text{m} \times 2\ \mu\text{m}$. Scale is adjusted to 0–10 nm in (D) for improved visualization of fibers of less than 10 nm.

Table 2. Surface Characterizations of Collagen Thin Films Deposited onto Hydrophobic Substrates

surface	mean roughness (nm)	mean fiber diameter (nm)	fiber surface area (nm^2) ^a	film thickness (nm)	collagen density (ng/mm^2)
CTF10	0.9 ± 0.1	3.9 ± 0.4	7600 ± 810	14 ± 2.4	4.2 ± 0.3
CTF100	1.7 ± 0.1	7.6 ± 1.1	12400 ± 740	15 ± 6.6	4.0 ± 0.3
CTF1000	2.8 ± 0.3	15.0 ± 2.0	42000 ± 10800	26 ± 7.7	7.1 ± 0.4
MC	1.6 ± 0.2	-	-	-	1.2 ± 0.1

^a Surface area of fibers contained from $2\ \mu\text{m} \times 2\ \mu\text{m}$ AFM image.

Table 2 is an increase in surface roughness, mean fiber diameter, and fiber surface area with concentration. Fiber surface area is reported from $2\ \mu\text{m} \times 2\ \mu\text{m}$ AFM images identical to those displayed Figure 3. This parameter in particular is reflective of the available binding sites for VWF proteins and platelets in later studies. Film thickness and ligand densities for each preparation are also listed. It is important to note that film thickness and ligand density calculation include collagen fibers that are buried underneath the surface layer of fibers and thus inaccessible for binding in flow assays. As such, we use surface area as the primary descriptor of CTFs. Fiber properties are not reported for MC substrates since these surfaces consist only of aggregated collagen monomers. The density of collagen for MC substrates is diminished compared to its CTF counterparts due to the lack of fiber polymerization at low pH. It is also important to note that all CTF measurements in Table 2 were taken after dehydration, as this is required for substrate bonding to microfluidic devices. In similar systems, dehydration of thin films has caused increased fiber packing, resulting in a $\sim 60\%$ decrease in film thickness and a $\sim 30\%$ decrease in surface roughness.^{21,35,38}

CTF can be grown on clean hydrophilic glass as well. CTF grown from $100\ \mu\text{g}/\text{mL}$ solutions on clean glass show a dense

film of collagen with a fibrillar morphology (Supporting Information Figure 1). Fiber sizes were $4.2 \pm 0.7\ \text{nm}$, which is 45% smaller in diameter compared to analogous CTF100 depositions on OTS substrates, an effect previously noted on hydrophilic surfaces.²⁰

Plasma VWF Binding to Collagen Thin Films. Prior to platelet adhesion at arterial shear stresses, VWF must be present on or bind to the subendothelial matrix. We measured the binding kinetics of plasma-derived VWF in buffer to each CTF and MC substrate listed in Table 1 at a wall shear rate of $5000\ \text{s}^{-1}$ using SPR. Under these flow conditions, VWF has been demonstrated to be functionally active in hemostasis.³⁹ As a control surface that accounts for nonspecific VWF adsorption to the surface, perfusion over BSA-passivated surfaces was also performed. VWF solutions were perfused at concentrations between $7.5\ \mu\text{g}/\text{mL}$ and $60\ \mu\text{g}/\text{mL}$.

Figure 4A shows representative plots of VWF association and dissociation dynamics to each CTF and MC substrate at VWF plasma levels ($10\ \mu\text{g}/\text{mL}$), and Table 3 displays the calculated association and disassociation rate constants and total VWF capture based on a 1:1 Langmuir model. This model has been widely used to fit plasma-derived VWF binding kinetics,^{30,40–42}

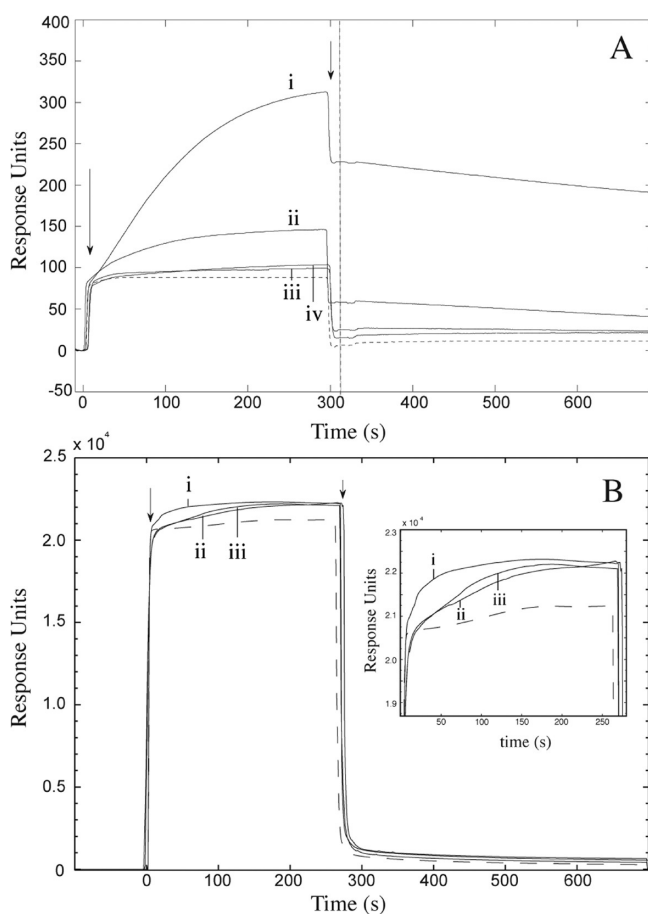


Figure 4. SPR analysis of VWF binding to collagen thin films. (A) $10\ \mu\text{g/mL}$ plasma VWF binding with (i) CTF1000, (ii) CTF100, (iii) CTF10, and (iv) MC substrates. The negative control (dashed line) represents perfusion of VWF over unligated surfaces. The vertical line represents the end-point capture levels of VWF after 5 min perfusion for each preparation. (B) $10\ \mu\text{g/mL}$ recombinant VWF binding with CTF1000 substrates. Recombinant VWF consisted of (i) wild type, (ii) Ser1731Thr mutant, and (iii) His1786Asp mutant. The negative control (dashed line) represents perfusion of cell culture media from a mock transfection containing no VWF. In both A and B, arrows represent the beginning and end of VWF perfusions. All surfaces were passivated with BSA after collagen depositions and all perfusions occurred for 5 min at a wall shear stress of $45\ \text{dyn/cm}^2$.

and enabled us to achieve fits with low average squared residual values ($\chi^2 < 15$ in all cases). A two-bond model similar to that used by Li and colleagues³⁰ gives similar trends in association rate constants as those in Table 3, but the model did not fit the data as well as the 1:1 Langmuir model as measured by the χ^2 parameter. Association rate constants of VWF to CTF substrates were on the order of 10^4 – $10^5\ \text{M}^{-1}\ \text{s}^{-1}$, significantly higher than reported values of $10^3\ \text{M}^{-1}\ \text{s}^{-1}$ for VWF perfusion over insoluble type I bovine collagen.³⁰ Dissociation rates for each preparation were on the order of $10^{-4}\ \text{s}^{-1}$, which is comparable to reported values for insoluble type I bovine fibrillar collagen.³⁰ We could not detect any VWF binding to IC by SPR, possibly because insoluble collagens do not conformally adsorb to the surface, but rather protrude into the lumen 20 – $100\ \mu\text{m}$.²⁹ One difference between our technique and the Li et al. study is that they covalently coupled the collagen to the SPR sensor, while we physically adsorbed the IC to a hydrophobic surface. Another VWF-collagen

Table 3. SPR Analysis of $5000\ \text{s}^{-1}$ VWF Perfusions over Collagen Thin Film Preparations

surface type	$k_a \times 10^5$ ($\text{M}^{-1}\ \text{s}^{-1}$) ^a	$k_d \times 10^{-4}$ (s^{-1}) ^a	VWF capture levels (pg/mm^2) ^b	χ^2
CTF10	0.3 ± 0.1	6.6 ± 2.0	23 ± 5	4.1
CTF100	1.8 ± 0.6	2.0 ± 0.1	110 ± 16	0.8
CTF1000	1.6 ± 0.3	2.8 ± 0.9	560 ± 42	13.1
MC	1.0 ± 0.2	7.3 ± 1.6	50 ± 4.5	0.1

^a k_a/k_d was measured by curve fitting using 1:1 Langmuir binding model after background subtraction of nonspecific VWF adsorption from binding curves. ^b Measured after 5 min perfusion of $10\ \mu\text{g/mL}$ VWF.

SPR study also found that measuring VWF binding to IC was not possible due to obstruction of the channel by collagen fibers.⁴³ Immunofluorescence staining of CTF substrates after VWF perfusion revealed a VWF layer of ball-and-string morphology typical of VWF extension at this shear stress (Supporting Information Figure 2).⁴⁴ No measurable VWF association was detected for collagen concentrations at $2\ \mu\text{g/mL}$ or lower.

Total VWF capture levels increased with increasing collagen solution concentrations. There was a 5-fold increase in VWF capture between CTF10 and CTF100 substrates, corresponding to the 60% increase in surface area from CTF10 to CTF100. Similarly, there was a 5-fold increase in VWF capture levels between CTF100 and CTF1000 substrates, corresponding to a 330% increase in surface area from CTF100 to CTF1000. This observation suggests that the increase in VWF association may be due to the increase in the surface area of collagen ligands available for binding (Table 2). Initial binding rates were independent of VWF concentration, so it is unlikely that binding was transport limited even at high ligand densities.

VWF also appears to associate with MC substrates, although the association rate and VWF adsorption capacity are diminished compared to its CTF1000 counterpart. This observation is likely due to the lower collagen density because of the lack of fiber formation and to the fact that VWF may require a collagen fibrillar structure to optimally bind under flow.¹⁶

Detection of VWF-Collagen Binding Deficiencies on Collagen Thin Films. To demonstrate the capacity of CTF substrates to discriminate against collagen-binding deficiencies in VWF, the binding kinetics of two recombinant VWF constructs, Ser1731Thr and His1786Asp, to CTF1000 substrates was monitored using SPR. Both constructs carry mutations in the A3 collagen-binding domain of VWF. In static collagen binding assays, Ser1731Thr constructs exhibit a 45% decrease in type I collagen binding affinity relative to wtVWF, while His1786Asp constructs exhibited $<1\%$ binding relative to wtVWF.²⁵ Samples containing $10\ \mu\text{g/mL}$ of recombinant wtVWF, Ser1731Thr, or His1786Asp constructs were perfused for 5 min in the SPR at $45\ \text{dyn/cm}^2$. As a negative control for nonspecific binding, cell media from a mock HEK293T transfection that contained no VWF was also perfused. Figure 4b shows the kinetics of VWF association and dissociation during perfusions from all samples. The magnitude of the resonance signal is higher in these mutant experiments (Figure 4B) compared to the plasma VWF (Figure 4A) because of the higher index of refraction of the cell media compared to PBS. The association and dissociation rates are summarized in Table 4. Relative to wtVWF, both Ser1731Thr and His1786Asp constructs show diminished

Table 4. SPR Analysis Recombinant VWF Perfusions over CTF1000 at of 5000 s^{-1}

recombinant VWF	$k_a \times 10^5 (\text{M}^{-1} \text{s}^{-1})^a$	$k_d \times 10^{-4} (\text{s}^{-1})^a$	χ^2
WT	23.6 ± 0.6	9.32 ± 1.22	147
S1713T	2.1 ± 0.2	0.44 ± 0.06	75
H1486D	5.1 ± 0.1	0.15 ± 0.03	128

^a k_a/k_d was measured by curve fitting using 1:1 Langmuir binding model after background subtraction of nonspecific VWF adsorption from binding curves.

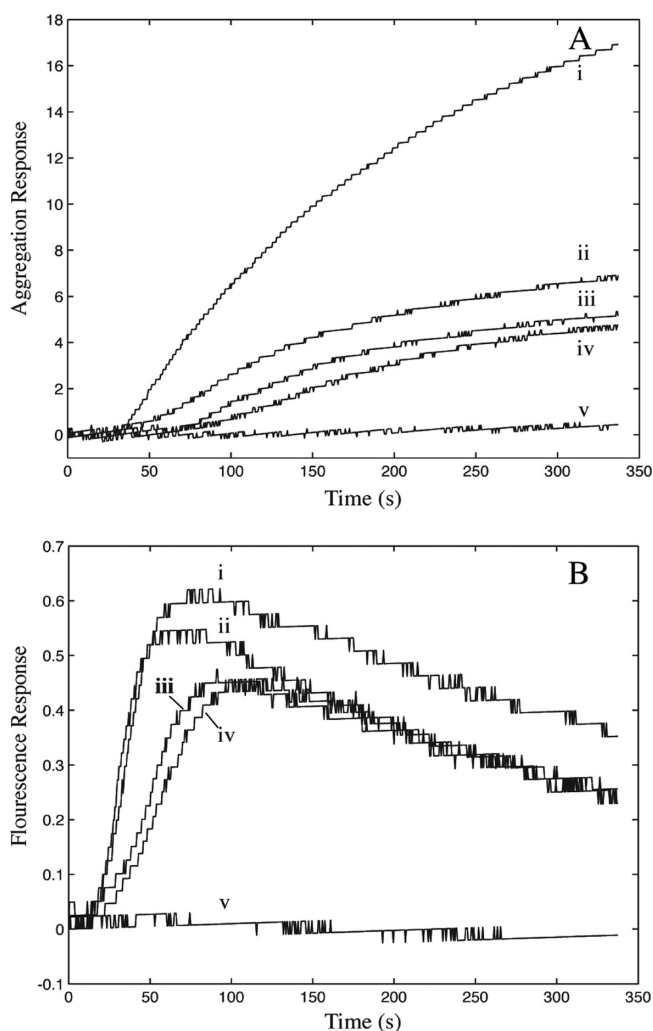


Figure 5. (A) Platelet aggregation and (B) platelet ATP release in citrated whole blood after addition of agonists: (i) $5 \mu\text{g}/\text{mL}$ fibrillar collagen, (ii) $15 \mu\text{g}/\text{mL}$ polymerized collagen, (iii) $5 \mu\text{g}/\text{mL}$ polymerized collagen, (iv) $2 \mu\text{g}/\text{mL}$ polymerized collagen, and (v) $15 \mu\text{g}/\text{mL}$ nonpolymerized collagen. Collagen solutions ii–iv were first polymerized for 1 h at $1000 \mu\text{g}/\text{mL}$ at room temperature, then diluted in $1 \times \text{PBS}$ to final concentration and added to whole blood.

association rates to the CTF substrate ($k_{a,S1731T}/k_{a,wt} = 0.09$, $k_{a,H1786D}/k_{a,wt} = 0.22$). The fact that His1786Asp constructs associate with the CTF substrates under flow but not in static assays is likely due to exposure of the A1 binding domain of VWF under critical shear stress, an effect that has been previously reported.^{25,40} These observations suggest that CTF

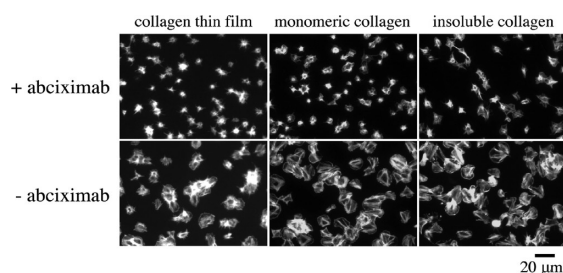


Figure 6. Representative images of platelet spreading on collagen surfaces. Washed human platelets ($2 \times 10^7 \text{ mL}$) were incubated over each substrate for 45 min at $37 \text{ }^\circ\text{C}$ in the presence or absence of $20 \mu\text{g}/\text{mL}$ abciximab, fixed, permeabilized, and stained with phalloidin-FITC.

preparations are sensitive to pathological collagen binding modifications in VWF, several of which are known to occur in qualitative defects of VWF such as VWD types 2A, 2B, and 2M.^{25,45,46}

Platelet Aggregation and Spreading on Collagen Thin Films. Platelet aggregometry was used to verify platelet activation by the collagen fibers present on CTF substrates. Aggregations were monitored in citrated whole blood using reconstituted collagen fibers as a platelet agonist. To prepare the agonist, type I bovine soluble collagen solutions were neutralized in $1 \times \text{PBS}$ for 1 h at $1000 \mu\text{g}/\text{mL}$, allowing for fiber reconstitution to occur in bulk solution. These experimental conditions are identical to those used in CTF1000 substrate preparation. As a negative control, an acid-solubilized collagen solution left in its monomeric form was also used as an agonist. This solution is identical to solutions used in MC substrate preparation. Finally, insoluble collagen used in IC substrates was used as a positive control agonist. Figure 5 shows the platelet aggregation response and the ATP generation due to dense granule release during platelet activation upon treatment with each agonist. Both plots show that platelets are activated and aggregate in a dose-dependent manner with the reconstituted fibers. Insoluble collagen induced a stronger response than the reconstituted fibers at equivalent concentrations. Collagen monomers were not capable of inducing aggregation due to their lack of a tertiary fibrillar structure required for engagement of platelet collagen receptors.⁴⁷ These results verify the functionality of CTFs toward platelet activation, as CTF surfaces contain similar reconstituted fibers to those used as an agonist in this experiment.

To evaluate the ability of CTF substrates to support platelet adhesion and activation, washed platelets were statically incubated over each substrate in Table 1 for 45 min. Platelets have been shown to interact with collagen surfaces via GPVI and integrin $\alpha_2\beta_1$. These receptors initiate platelet signaling downstream of collagen binding, eventually leading to activation of the integrin $\alpha_{IIb}\beta_3$. Sustained “outside-in” signaling via $\alpha_{IIb}\beta_3$ results in platelet spreading.⁴⁸ As illustrated in Figure 6, platelet adhesion to and the degree of spreading on CTF surfaces was comparable to that observed on IC surfaces. Furthermore, inhibition of $\alpha_{IIb}\beta_3$ with abciximab abrogated platelet spreading on each surface. Minimal platelet adhesion was observed on control BSA surfaces. These results demonstrate the ability of CTF substrates to promote both platelet adhesion and activation under static conditions. The platelet adhesion and spreading observed on MC substrates are consistent with previous reports that collagen monomers support static, $\alpha_2\beta_1$ -mediated platelet adhesion and spreading.^{49,50}

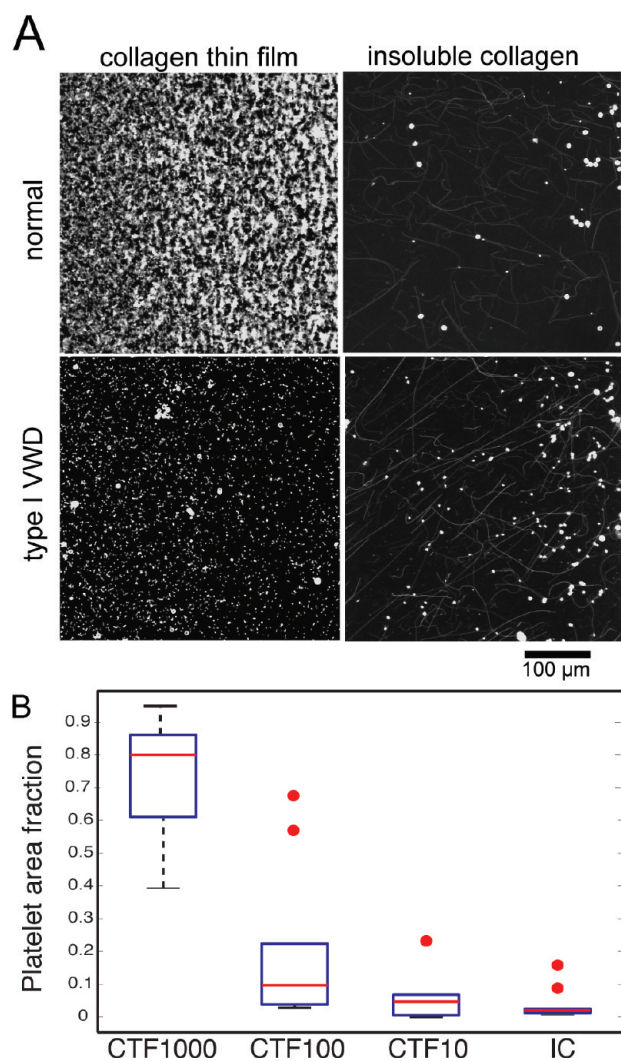


Figure 7. (A) Representative confocal microscope images of anti-CD41-Alexa Fluor 647 labeled platelets after 5 min of perfusion of whole blood taken from healthy donors or a type I VWD patient. Whole blood was perfused at a 1000 s^{-1} wall shear rate over CTF1000 or IC substrates. (B) Box plot of platelet area fraction on CTF1000, CTF100, CTF10, and IC for healthy donors ($n = 10$). Red circles represent outliers.

Platelet Adhesion to Collagen Thin Films under Arterial Shear Stress. The previous sections show that CTFs are a homogeneous substrate at the micrometer length scale and support VWF-collagen binding and platelet activation. In this section, we present data to show that CTFs can be used in flow assays (Figure 1) to support platelet adhesion under flow and to distinguish platelet adhesion between healthy controls and VWD patients. We measured platelet adhesion to CTF substrates following a 5 min perfusion at 1000 s^{-1} (32 dyn/cm^2) for healthy donors and type 1 VWD patients. Experiments were performed at a shear stress that requires VWF for platelet adhesion to collagen. To isolate platelet adhesion from aggregation, we inhibited fibrinogen-mediated platelet–platelet binding with abciximab, an integrin $\alpha_{\text{IIb}}\beta_3$ antagonist. Whole blood perfusions over MC and IC substrates were performed as controls. Figure 7 shows representative end point images and surface coverage levels of platelets adhered to CTF1000 and IC

Table 5. Platelet Fractional Surface Coverage over Each Collagen Preparation Following 5 min Perfusions of Whole Blood at 1000 s^{-1}

donor	CTF 1000	CTF 100	CTF 10	MC	IC
1 ^a	0.86 ± 0.04	0.68 ± 0.09	0.23 ± 0.05	0.03 ± 0.01	- ^c
2 ^a	0.81 ± 0.03	0.04 ± 0.006	0.03 ± 0.007	-	0.01 ± 0.01
3 ^a	0.81 ± 0.08	0.03 ± 0.002	0.01 ± 0.003	0.03 ± 0.01	0.02 ± 0.01
4 ^a	0.51 ± 0.20	0.56 ± 0.12	0.06 ± 0.01	0.02 ± 0.01	-
5 ^a	0.79 ± 0.02	0.17 ± 0.04	0.06 ± 0.02	-	0.02 ± 0.02
6 ^a	0.39 ± 0.12	0.07 ± 0.04	-	-	0.02 ± 0.01
7 ^a	0.95 ± 0.03	0.22 ± 0.10	0.06 ± 0.03	-	0.16 ± 0.03
8 ^a	0.61 ± 0.06	0.03 ± 0.01	0.07 ± 0.03	-	0.02 ± 0.01
9 ^a	0.88 ± 0.05	0.12 ± 0.04	-	-	0.09 ± 0.04
10 ^a	0.77 ± 0.03	0.04 ± 0.02	0.02 ± 0.01	-	0.02 ± 0.01
11 ^b	0.08 ± 0.05	0.02 ± 0.008	-	-	0.01 ± 0.01
12 ^b	0.24 ± 0.06	0.03 ± 0.006	0.03 ± 0.02	-	0.04 ± 0.03

^a Healthy donors. ^b Type I VWD patients. ^c Dash (-) means less than 0.01 fractional surface coverage.

substrates after whole blood perfusions from ten healthy donors (donors 1–10) and two type 1 VWD patients (donors 11–12) with plasma VWF levels of $3.83 \mu\text{g/mL}$ (donor 11) and $1.25 \mu\text{g/mL}$ (donor 12). A normal plasma VWF level is $\sim 10 \mu\text{g/mL}$. There was a significant difference ($p < 0.01$) in platelet adhesion between CTF1000 and the other three substrates (CTF10, CTF100, and IC) among healthy donors. VWD patients had platelet surface coverages of 0.08 ± 0.05 (donor 11) and 0.24 ± 0.06 (donor 12), which are almost 3 standard deviations outside the platelet surface coverage (0.74 ± 0.17) among the healthy donors. On IC substrates, platelets adhered directly to large ($>100 \text{ nm}$) insoluble fibers and in the regions between fibers as well. However, there was a lack of discrimination between normal and VWD patients.

Table 5 gives a summary of fractional platelet surface coverage on all substrates. CTF100 and CTF10 substrates, which contained smaller fibers and lower surface areas, supported lower platelet surface coverage compared to CTF1000 substrates for each donor. Average fractional surface coverage on CTF100 and CTF10 across the ten healthy donors showed high levels of variance (0.20 ± 0.23 and 0.06 ± 0.07 , respectively). Even if the outliers (Figure 7B) are ignored, the standard deviation in the data is comparable to the mean. MC substrates consistently showed fractional platelet coverage of less than 0.05 across healthy donors. This result verifies the requirement of collagen monomers to polymerize into a supramolecular structure for the formation of collagen epitopes specific to platelet integrin $\alpha_2\beta_1$ (GFOGER) and glycoprotein VI (GPO) that allow for firm adhesion under flow.^{1,51,52} Although platelets can spread on MC substrates (Figure 6), MC substrates cannot support firm adhesion under flow, suggesting that the kinetics of binding to or signaling downstream of MC binding is slower than that for polymerized collagen.

DISCUSSION

The objective of this study was to characterize CTFs as substrates for measuring platelet recruitment under flow. The essential functions of collagen in thrombus formation are to bind VWF and act as an adhesive and signaling ligand for platelets. We

found that CTFs can bind VWF at arterial shear stress and can distinguish between wild-type VWF and collagen binding-deficient VWF mutants. Platelet adhesion at arterial shear stress is also supported on CTFs in a surface ligand density-dependent manner. At high ligand densities, we observed diminished platelet adhesion with whole blood from VWD patients compared to healthy controls. These results suggest that CTF may be a good candidate substrate for diagnosing and quantifying platelet adhesion disorders.

The conventional collagen substrates for flow assays are types I and III insoluble native fibers from nonhuman sources. These insoluble collagens (IC) are potent platelet agonists that induce strong outside-in signaling through platelet collagen receptors. Reconstituted fibers from acid-solubilized collagens, such as those used to make CTF substrates in this study, are not as strong of a platelet agonist.^{16,53} In aggregometry studies, we found that, at the same concentration (5 $\mu\text{g}/\text{mL}$), IC is approximately 50% more potent than CTF fibers in inducing platelet activation as measured by ATP release. Platelets adhered to and spread similarly on IC and CTF. These measurements suggest that CTF are capable of activating platelets, although perhaps not with the same potency of IC.

A direct comparison of surface-bound IC and CTF becomes more difficult because the surface density of fibers appears to be significantly different between the two preparations (Figure 2). The IC surfaces (Figure 2C) have both large fibers O(100 nm) and small fibers O(10 nm), and the relative density of these features varies between preparations. We observed that platelets adhere not only to large fibers that are optically visible, but also in the spaces between larger fibers, suggesting that these small fibers may promote platelet adhesion. Since the relative density of the large and small fibers varies between preparations in our hands, this makes this substrate nonideal for a clinical setting. In addition, there is evidence that IC contains significant amounts of endogenous VWF,¹⁸ which may block binding sites for human VWF during flow assays. Nevertheless, a comparison between platelet adhesion under flow on IC adsorbed from 100 $\mu\text{g}/\text{mL}$ solutions and CTF grown from 100 $\mu\text{g}/\text{mL}$ solutions (CTF100) shows inconsistent results. In five of the ten healthy donors, platelet surface coverage was more than 2-fold greater on CTF100 substrates. In the other five healthy donors and both VWD patients, the surface coverage levels were higher on CTF100 substrates, but the difference was statistically insignificant.

A distinct advantage of using the CTF preparation is the ability to tune the surface ligand density. This was demonstrated in both VWF and platelet adhesion studies. For VWF binding, data in Table 3 suggest that fiber surface area can be used to modulate the amount of VWF association. This feature may be particularly useful in further studies with samples from individuals with VWD. For example, some cases of type 2 VWD are characterized by decreases in high molecular weight multimers that are thought to play an essential role in VWF affinity to collagen.¹⁵ Such VWF mutants may not be detected by conventional, static clinical laboratory assays, but perhaps could be effectively identified by increasing the collagen surface area in a flow-based assay, adding sensitivity and specificity in characterizing the effect of these mutations on hemostatic function. In this report, we have demonstrated this strategy by using high surface area CTF1000 substrates to discriminate collagen-binding deficiencies in VWF.

Similarly for platelet adhesion studies, tuning the surface area was important to achieving reproducible results. The highest

platelet adhesion and the lowest variability were observed on CTF1000. CTF1000 was the only surface without outliers (>2.7 standard deviations) among the healthy controls. More importantly for diagnostic applications, CTF1000 was the only surface on which platelet surface coverage levels were statistically different between healthy controls and VWD patients. It is not surprising that there is significant variation on CTFs and IC given the tremendous variability in hematocrit (0.35–0.50), platelet count (150 000–300 000/ μL), VWF levels, and platelet collagen receptor expression between individuals. Plasma VWF levels and the density of the collagen receptor $\alpha_2\beta_1$ correlate with platelet adhesion and aggregation on collagen.^{54–56} Our data suggest that some of this variability can be mitigated at high collagen densities in order to distinguish normal and VWD samples.

The relatively small fibers formed on hydrophilic substrates and CTF10 are similar to those seen in previous studies.^{38,57} It is possible that these fibers are not fibrillar at all given that the diameter of tropocollagen is 1.5 nm⁵⁸ and the thickness of these fibers is ~ 4 nm. This may explain why these substrates have different binding kinetics with VWF and lower platelet adhesion compared to CTF100 and CTF1000.

It is important to draw a distinction between the microfluidic channels used in this study and the larger and more widely used parallel plate flow assays. In parallel plate assays, the heterogeneity of adsorbed IC at the submicrometer scale may not be significant when averaged over a large area of ~ 100 mm². However, as the flow assay is scaled down to smaller microfluidic channels, the tolerance for heterogeneity in collagen fiber distribution decreases. In our experience with microfluidic flow assays using both human and murine blood, the heterogeneity in fiber size and density with IC adsorption confound data analysis.⁸ Regardless of channel size, there is growing appreciation for the need of a repeatable collagen substrate since there is already high variability in the endogenous properties of blood among individuals.^{10,17}

An alternative strategy to reconstituted fibers that may lend itself to a microfluidic format is synthetic collagen related peptides. Pugh and colleagues showed that an ensemble of synthetic peptides can support platelet adhesion and aggregation over the range of physiological shear rates (100–3000 s⁻¹).²⁹ A critique of synthetic peptides, as well as the reconstituted fibers used in this study, is that they do not accurately represent the *in vivo* subendothelium, which is a milieu of extracellular matrix proteins and lipids. Mimicking the composition of the subendothelium may be important for investigating fundamental biological mechanisms, but for the development of a clinical assay, strict control over substrate properties is essential for eliminating additional confounding factors in the interpretation of the results.

CONCLUSIONS

There is an unmet need for a homogeneous, repeatable adhesive substrate for platelet adhesion flow assays, and considerable debate surrounds identifying the best candidate. In this report, we have demonstrated the utility and potential advantages of CTF substrates for application to platelet adhesion flow assays. This approach relies on the formation of reconstituted collagen fibers at the solid–liquid interface during thin film deposition. We have shown that the homogeneity in the resulting fiber size and surface coverage on a submicrometer scale compare favorably to traditional IC substrates, especially for applications

in microfluidic formats. The functionality of CTF toward VWF and platelets during perfusions under high shear stresses found in the arterial system has been verified. Furthermore, we have demonstrated that thin film properties can be manipulated to influence the degree of VWF adsorption and platelet adhesion. In application of CTF implementation in a clinical diagnostic assay, we have shown that reproducible levels of platelet adhesion are achieved among normal donors when CTFs contain above a threshold collagen ligand density. Finally, CTF substrates are sensitive to dysfunctions in VWF-collagen binding and platelet-collagen adhesion that are characteristic of von Willebrand disease.

■ ASSOCIATED CONTENT

S Supporting Information. Additional figures of collagen thin films on clean glass and immunofluorescent images of VWF on collagen thin films. This material is available free of charge via the Internet at <http://pubs.acs.org>.

■ AUTHOR INFORMATION

Corresponding Author

*E-mail: kneeves@mines.edu, Tel: 01-303-273-3191, Fax: 01-303-273-3730.

■ ACKNOWLEDGMENT

This work was supported by a Scientist Development Grant (K.B.N.) and a Postdoctoral Fellowship (R.R.H) from the American Heart Association, the National Heart, Lung, and Blood Institute (HL100333), the Colorado Office of Economic Development and International Trade, and the Boettcher Foundation's Webb-Waring Biomedical Research Award. The authors would like to thank Dr. Veronica Flood of the BloodCenter of Wisconsin for providing recombinant VWF constructs and Megan Sumner for expert technical assistance during the platelet aggregometry studies.

■ REFERENCES

- (1) Farndale, R. W.; Sixma, J. J.; Barnes, M. J.; de Groot, P. G. *J. Thromb. Haemost.* **2004**, *2*, 561–73.
- (2) Ginsburg, D. *Haemophilia* **1999**, *5*, 19–27.
- (3) Sakariassen, K. S.; Aarts, P. A. M. M.; Degroot, P. G.; Houdijk, W. P. M.; Sixma, J. J. *Lab. Clin. Med.* **1983**, *102*, 522–535.
- (4) Turitto, V. T.; Weiss, H. J.; Baumgartner, H. R. *J. Clin. Invest.* **1984**, *74*, 1730–41.
- (5) Fressinaud, E.; Sakariassen, K. S.; Rothschild, C.; Baumgartner, H. R.; Meyer, D. *Blood* **1992**, *80*, 988–994.
- (6) Usami, S.; Chen, H. H.; Zhao, Y. H.; Chien, S.; Skalak, R. *Ann. Biomed. Eng.* **1993**, *21*, 77–83.
- (7) Barstad, R. M.; Roald, H. E.; Cui, Y. W.; Turitto, V. T.; Sarariassen, K. S. *Arterioscler. Thromb.* **1994**, *14*, 1984–1991.
- (8) Neeves, K. B.; Maloney, S. F.; Fong, K. P.; Schmaier, A. A.; Kahn, M. L.; Brass, L. F.; Diamond, S. L. *J. Thromb. Haemost.* **2008**, *6*, 2193–2201.
- (9) Gutierrez, E.; Petrich, B. G.; Shattil, S. J.; Ginsberg, M. H.; Grosman, A.; Kasirer-Friede, A. *Lab Chip* **2008**, *8*, 1486.
- (10) Zwaginga, J. J.; Sakariassen, K. S.; King, M. R.; Diacovo, T. G.; Grabowski, E. F.; Nash, G.; Hoylaerts, M.; Heemskerk, J. W. M. *J. Thromb. Haemost.* **2007**, *5*, 2547–2549.
- (11) Savage, B.; Almus-Jacobs, F.; Ruggeri, Z. M. *Cell* **1998**, *94*, 657–66.
- (12) White-Adams, T. C.; Berny, M. A.; Patel, I. A.; Tucker, E. I.; Gailani, D.; Gruber, A.; McCarty, O. J. T. *J. Thromb. Haemost.* **2010**, *8*, 1295–1301.
- (13) Kuijpers, M.; Schulte, V.; Bergmeier, W.; Lindhout, T.; Brakebusch, C.; Offermanns, S.; Fassler, R.; Heemskerk, J.; Nieswandt, B. *FASEB J.* **2003**, *17*, 685–.
- (14) Sixma, J. J.; van Zanten, G. H.; Huizinga, E. G.; van der Plas, R. M.; Verkley, M.; Wu, Y. P.; Gros, P.; de Groot, P. G. *Thromb. Haemost.* **1997**, *78*, 434–8.
- (15) Sadler, J. *Annu. Rev. Biochem.* **1998**, *67*, 395–424.
- (16) Savage, B.; Ginsberg, M.; Ruggeri, Z. *Blood* **1999**, *94*, 2704–2715.
- (17) Heemskerk, J. W.; Sakariassen, K. S.; Zwaginga, J. J.; Brass, L. F.; Jackson, S. P. *J. Thromb. Haemost.* **2011**.
- (18) Bernardo, A.; Bergeron, A. L.; Sun, C. W.; Guchhait, P.; Cruz, M. A.; López, J. A.; Dong, J.-F. *J. Thromb. Haemost.* **2004**, *2*, 660–9.
- (19) Dupont-Gillain, C.; Rouxhet, P. *Langmuir* **2001**, *17*, 7261–7266.
- (20) Elliott, J. T.; Woodward, J. T.; Umarji, A.; Mei, Y.; Tona, A. *Biomaterials* **2007**, *28*, 576–585.
- (21) Dupont-Gillain, C.; Pamula, E.; Denis, F.; De Cupere, V.; Dufrene, Y.; Rouxhet, P. *J. Mater. Sci.: Mater. Med.* **2004**, *15*, 347–353.
- (22) Elliott, J. T.; Tona, A.; Woodward, J. T.; Jones, P. L.; Plant, A. L. *Langmuir* **2003**, *19*, 1506–1514.
- (23) Keresztes, Z.; Rouxhet, P. G.; Remacle, C.; Dupont-Gillain, C. *J. Biomed. Mater. Res. A* **2006**, *76*, 223–33.
- (24) Langenbach, K. J.; Elliott, J. T.; Tona, A.; McDaniel, D.; Plant, A. L. *BMC Biotechnol.* **2006**, *6*, 14.
- (25) Flood, V. H.; Lederman, C. A.; Wren, J. S.; Christopherson, P. A.; Friedman, K. D.; Hoffmann, R. G.; Montgomery, R. R. *J. Thromb. Haemost.* **2010**, *8*, 1431–1433.
- (26) Gurdak, E.; Rouxhet, P.; Dupont-Gillain, C. *Colloid Surf., B* **2006**, *52*, 76–88.
- (27) Wasserman, S.; Tao, Y.; Whitesides, G. *Langmuir* **1989**, *5*, 1074–1087.
- (28) Jeenanong, A.; Kawaguchi, H. *Colloid Surf., A* **2007**, *302*, 403–410.
- (29) Pugh, N.; Simpson, A. M. C.; Smethurst, P. A.; de Groot, P. G.; Raynal, N.; Farndale, R. W. *Blood* **2010**, *115*, 5069–5079.
- (30) Li, F.; Moake, J.; McIntire, L. *Ann. Biomed. Eng.* **2002**, *30*, 1107–1116.
- (31) Rice, R. V.; Casassa, E. F.; Kerwin, R. E.; Maser, M. D. *Arch. Biochem. Biophys.* **1964**, *105*, 409–23.
- (32) McCarty, O. J. T.; Zhao, Y.; Andrew, N.; Machesky, L. M.; Staunton, D.; Frampton, J.; Watson, S. P. *J. Thromb. Haemost.* **2004**, *2*, 1823–1833.
- (33) McDonald, J. C.; Duffy, D. C.; Anderson, J. R.; Chiu, D. T.; Wu, H.; Schueller, O. J.; Whitesides, G. M. *Electrophoresis* **2000**, *21*, 27–40.
- (34) Zack, G. W.; Rogers, W. E.; Latt, S. A. *J. Histochem. Cytochem.* **1977**, *25*, 741–53.
- (35) Jacquemart, I.; Pamua, E.; De Cupere, V.; Rouxhet, P.; Dupont-Gillain, C. *J. Colloid Interface Sci.* **2004**, *278*, 63–70.
- (36) Pareti, F. I.; Niiya, K.; McPherson, J. M.; Ruggeri, Z. M. *J. Biol. Chem.* **1987**, *262*, 13835–41.
- (37) Auger, J.; Kuijpers, M.; Senis, Y.; Watson, S.; Heemskerk, J. *FASEB J* **2005**, *19*, 825–.
- (38) Chung, K.-H.; Bhadriraju, K.; Spurlin, T. A.; Cook, R. F.; Plant, A. L. *Langmuir* **2010**, *26*, 3629–3636.
- (39) Schneider, S. W.; Nuschele, S.; Wixforth, A.; Gorzelanny, C.; Alexander-Katz, A.; Netz, R. R.; Schneider, M. F. *Proc. Natl. Acad. Sci. U. S. A.* **2007**, *104*, 7899–903.
- (40) Bonnefoy, A.; Romijn, R. A.; Vandervoort, P. A. H.; VAN Rompaey, I.; Vermynen, J.; Hoylaerts, M. F. *J. Thromb. Haemost.* **2006**, *4*, 2151–61.
- (41) Romijn, R. A.; Westein, E.; Bouma, B.; Schiphorst, M. E.; Sixma, J. J.; Lenting, P. J.; Huizinga, E. G. *J. Biol. Chem.* **2003**, *278*, 15035–15039.
- (42) Serrano, S. M. T.; Jia, L. G.; Wang, D. Y.; Shannon, J. D.; Fox, J. W. *Biochem. J.* **2005**, *391*, 69–76.

- (43) Romijn, R. A.; Westein, E.; Bouma, B.; Schiphorst, M. E.; Sixma, J. J.; Lenting, P. J.; Huizinga, E. G. *J. Biol. Chem.* **2003**, *278*, 15035–9.
- (44) Siedlecki, C. A.; Lestini, B. J.; Kottke-Marchant, K. K.; Eppell, S. J.; Wilson, D. L.; Marchant, R. E. *Blood* **1996**, *88*, 2939–50.
- (45) Ribba, A. S.; Loisel, I.; Lavergne, J. M.; Juhan-Vague, I.; Obert, B.; Cherel, G.; Meyer, D.; Girma, J. P. *Thromb. Haemost.* **2001**, *86*, 848–854.
- (46) Baronciani, L.; Federici, A. B.; Beretta, M.; Cozzi, G.; Canciani, M. T.; Mannucci, P. M. *J. Thromb. Haemost.* **2005**, *3*, 2689–2694.
- (47) Farndale, R. W. *Blood Cell Mol. Dis.* **2006**, *36*, 162–165.
- (48) Shattil, S. J.; Kashiwagi, H.; Pampori, N. *Blood* **1998**, *91*, 2645–2657.
- (49) Morton, L. F.; Peachey, A. R.; Zijenah, L. S.; Goodall, A. H.; Humphries, M. J.; Barnes, M. J. *Biochem. J.* **1994**, *299*, 791–797.
- (50) White, T. C.; Berny, M. A.; Robinson, D. K.; Yin, H.; DeGrado, W. F.; Hanson, S. R.; McCarty, O. J. T. *FEBS J.* **2007**, *274*, 1481–1491.
- (51) O'Connor, M. N.; Smethurst, P. A.; Davies, L. W.; Joutsikorhonen, L.; Onley, D. J.; Herr, A. B.; Farndale, R. W.; Ouwehand, W. H. *J. Biol. Chem.* **2006**, *281*, 33505–33510.
- (52) Polanowska-Grabowska, R. *Arteriosclerosis, Thrombosis, Vascular Biology* **2003**, *23*, 1934–1940.
- (53) Houdijk, W. P.; Sakariassen, K. S.; Nievelstein, P. F.; Sixma, J. J. *J. Clin. Invest.* **1985**, *75*, 531–40.
- (54) Kritzik, M.; Savage, B.; Nugent, D. J.; Santoso, S.; Ruggeri, Z. M.; Kunicki, T. J. *Blood* **1998**, *92*, 2382–8.
- (55) Di Paola, J.; Federici, A. B.; Mannucci, P. M.; Canciani, M. T.; Kritzik, M.; Kunicki, T. J.; Nugent, D. *Blood* **1999**, *93*, 3578–82.
- (56) Roest, M.; Sixma, J. J.; Wu, Y. P.; Ijsseldijk, M. J.; Tempelman, M.; Slootweg, P. J.; de Groot, P. G.; van Zanten, G. H. *Blood* **2000**, *96*, 1433–7.
- (57) Gale, M.; Pollanen, M. S.; Markiewicz, P.; Goh, M. C. *Biophys. J.* **1995**, *68*, 2124–8.
- (58) Fraser, R. D.; MacRae, T. P.; Suzuki, E. *J. Mol. Biol.* **1979**, *129*, 463–81.